

A coupling model for fluid-structure interaction applications with free-surface flows and rigid-bodies

Mateus Guimarães Tonin¹, Alexandre Luis Braun¹

¹*Programa de Pós-Graduação em Engenharia Civil, Universidade Federal do Rio Grande do Sul
Av. Osvaldo Aranha 99, 90035-190, Porto Alegre - RS, Brazil
mateus.tonin@ufrgs.br, alexandre.braun@ufrgs.br*

Abstract. In the present work, a formulation based on the Characteristic Based Split (CBS) method is proposed for applications in fluid-structure interaction (FSI) and free-surface flow problems. The flow fundamental equations are discretized here using the CBS method in the context of the Finite Element Method (FEM), where linear tetrahedral elements are employed. A semi-implicit scheme is used, where the momentum equations are solved explicitly while the mass equation is solved implicitly through a Poisson equation. FSI is taken into account considering a partitioned coupling model and the rigid-body approach, considering an Arbitrary Lagrangian-Eulerian (ALE) kinematic formulation. The resulting dynamic equilibrium equation is solved using the Generalized- α method. Free-surface flows are analyzed using the Level Set Method (LSM), considering a two-phase medium. Classic free-surface and FSI problems are simulated in order to evaluate the present formulation, comparing results obtained here with experimental results and predictions obtained with other numerical formulations available. It is concluded that the proposed numerical tool is able to obtain results consistent with the phenomena involved.

Keywords: Characteristic Based Split (CBS); Fluid-Structure Interaction (FSI); Free-Surface Flows.

1 Introduction

Floating structures have been used in different areas of Engineering. There are a lot of applications in this area, including ship hydrodynamics (Biran and López-Pulido [1]), offshore structures (Karimirad et al. [2]), and even buildings, bridges and harbors (Wang and Wang [3]). All these applications cannot be imagined without an intensive use of computers and numerical methods (Sharma et al. [4]).

Unfortunately, the numerical treatment of Fluid-Structure Interaction (FSI) problems, especially those in the presence of free surfaces may pose several modeling challenges, as pointed by Sanders et al. [5] and Calderer et al. [6]. As a result, many different types of methodologies and ways of modeling the problem can be developed. Some of them are listed in Sharma et al. [4], as well as some key challenges in computer applications for ship and floating structure design and analysis.

In this work, a numerical model is proposed considering the Navier-Stokes and mass conservation equations, which are discretized using the semi-implicit form of the Characteristic-based Split (CBS) Method for incompressible flows and Newtonian fluids. In the present formulation, the momentum equations are solved explicitly while the mass equation is solved implicitly through a Poisson equation. Free surfaces are modeled using the Level Set Method (LSM) and a two-phase medium approach for the flow field. The system of flow equations obtained here is discretized using the Finite Element Method (FEM), where linear tetrahedral finite elements are utilized. Finally, the fluid-structure interaction (FSI) problem is solved using a partitioned coupling model and a rigid-body approach for the immersed structure.

2 Flow Fundamental Equations and Numerical Model

2.1 Flow Dynamics and Free Surface Modeling

The momentum and mass conservation equations are utilized here considering the incompressible flow hypothesis and an arbitrary Lagrangian-Eulerian description (Zienkiewicz et al. [7]). By applying the semi-implicit CBS Method to the system of flow fundamental equations, one obtains (see Nithiarasu et al. [8]):

$$\Delta v_i^* = \Delta t \left[-(v_j^n - w_j^n) \frac{\partial v_i^n}{\partial x_j} + \frac{1}{\rho} \frac{\partial \tau_{ij}^n}{\partial x_j} + g_i \right] + \frac{\Delta t^2}{2} (v_k^n - w_k^n) \frac{\partial}{\partial x_k} \left[(v_j^n - w_j^n) \frac{\partial v_i^n}{\partial x_j} \right], \quad (1)$$

$$\Delta t \theta_1 \theta_2 \frac{\partial^2 \Delta p}{\partial x_i^2} = \rho \frac{\partial v_i^n}{\partial x_i} + \rho \theta_1 \frac{\partial \Delta v_i^*}{\partial x_i} - \Delta t \theta_1 \frac{\partial^2 p^n}{\partial x_i^2}, \quad (2)$$

$$\Delta v_i^{**} = -\Delta t \frac{1}{\rho} \frac{\partial p^{n+\theta_2}}{\partial x_i} + \frac{\Delta t^2}{2} v_k^n \frac{\partial}{\partial x_k} \left[\frac{1}{\rho} \frac{\partial p^n}{\partial x_i} \right]. \quad (3)$$

where x_j denote coordinate directions in an orthogonal Cartesian coordinate system, v_i are components of the flow velocity vector, w_i are components of the mesh velocity vector, p is the pressure, τ_{ij} are components of the viscous stress tensor, g_i are components of the gravity acceleration vector, ρ is the fluid specific mass, Δt is the time increment, while θ_1 and θ_2 are model parameters with values varying from 0.5 to 1.0 and 0 to 1, respectively. Notice that 3rd order terms or higher are disregarded and a split operation is performed considering the momentum equations, such that the flow velocity field is decomposed into $\Delta v_i = \Delta v_i^* + \Delta v_i^{**}$ in a time interval $[t_n, t_{n+1}]$. The FEM is then applied to the discretized equations to solve the flow problem, where linear tetrahedral elements are utilized.

For free surface modeling, a biphasic flow approach is adopted using the Level-Set Method proposed by Osher and Sethian [9]. In this method, a scalar distance function with signal ϕ is used, which is determined with the following equation:

$$\frac{\partial \phi}{\partial t} + v_j \frac{\partial \phi}{\partial x_j} = 0. \quad (4)$$

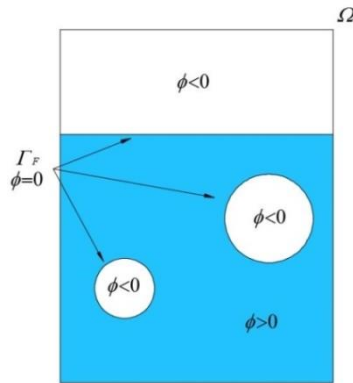


Figure 1. Level Set function to identify ascending gas bubbles in a fluid (Pochet et al. [10])

Figure 1 shows a typical scalar field ϕ , where one can observe that the total volume (area) Ω is composed by two fluids: a liquid (water) region, where $\phi > 0$, and a gas (air) region, where $\phi < 0$, while the interface is defined by $\phi = 0$ and represented by the boundary lines Γ_F . The fluid physical properties are then defined as functions of ϕ , as follows:

$$\rho(\phi) = \rho_1 + (\rho_2 - \rho_1) H(\phi). \quad (5)$$

being ρ_1 and ρ_2 the fluid densities corresponding to fluids 1 and 2, respectively, and $H(\phi)$ is a ‘‘smoothed’’

Heaviside function, given by:

$$H(\phi) = \begin{cases} 0 & \text{para } \phi < -\varepsilon \\ \frac{1}{2} \left[1 + \frac{\phi}{\varepsilon} + \frac{1}{\pi} \text{sen} \left(\frac{\pi\phi}{\varepsilon} \right) \right] & \text{para } |\phi| \leq \varepsilon. \\ 1 & \text{para } \phi > \varepsilon \end{cases} \quad (6)$$

where ε is the half-thickness of the transition zone, normally defined as $\varepsilon = \alpha_{LS} \Delta x$, where Δx is the characteristic dimension of an element in the interface region and α_{LS} is a model parameter with values varying between 1 and 2.

The numerical solution of Eq. (4) does not guarantee that ϕ will remain as a distance function (i.e. $|\nabla\phi| = 1$), thus a reinitialization procedure is necessary to ensure this condition (see Sussman et al. [11]):

$$\frac{\partial\psi}{\partial\tau} + S(\psi_0)(|\nabla\psi| - 1) = 0, \quad (7)$$

where ψ is an auxiliary function, whose initial position is given by:

$$\psi_0(\mathbf{x}, \tau = 0) = \phi(\mathbf{x}, t), \quad (8)$$

while the smoothed function $S(\psi_0)$ is given by:

$$S(\psi_0) = \frac{\psi_0}{\sqrt{\psi_0^2 + (|\nabla\psi_0|\varepsilon)^2}}, \quad (9)$$

where τ is an artificial time variable from which one can define a steady state for ψ in each time instant t of the numerical analysis. The steady state is usually obtained up to $\varepsilon/\Delta\tau$ iterations, being $\Delta\tau$ defined by:

$$\Delta\tau \leq \chi \frac{\Delta x^2}{\varepsilon}, \quad (10)$$

where χ is a safety factor that assumes values between 0 and 1.

2.2 Rigid Body Dynamics and FSI Modeling

The structure is idealized in this work as a rigid body, which is a reasonable assumption, considering that the displacements and rotations generated by the flow are much larger than the body deformations. The dynamic equilibrium equation of the body is given by:

$$\mathbf{M}_S \ddot{\mathbf{U}}_S^c + \mathbf{C}_S \dot{\mathbf{U}}_S^c + \mathbf{K}_S \mathbf{U}_S^c = \mathbf{Q}_S^c. \quad (11)$$

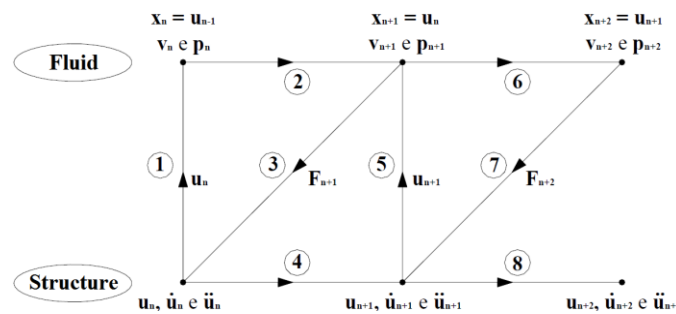


Figure 2. Solution algorithm for a FSI problem (Braun [12]).

where \mathbf{M}_S is the mass matrix, \mathbf{C}_S is the damping matrix, \mathbf{K}_S is the stiffness matrix and \mathbf{U}_S^c , $\dot{\mathbf{U}}_S^c$ and $\ddot{\mathbf{U}}_S^c$ are the generalized displacement, velocity and acceleration vectors, respectively, while \mathbf{Q}_S^c is the force vector. The subscript S is related to the structure, and the superscript c is related to the center of gravity of the structure.

A partitioned scheme is utilized here for the FSI coupling, where the flow and structural domains are solved sequentially by imposing kinematic compatibility and equilibrium conditions at the fluid-structure interface. A flowchart of the FSI algorithm adopted in this work is presented in Figure 2. Additional information on the FSI model employed in the present investigation may be found in Braun [12].

3 Applications

3.1 Broken Dam Problem

The present example is utilized to verify the numerical model proposed in this work when flow problems with free surfaces are considered. This application was studied first by Martin and Moyce [13] using experimental techniques. In this problem, a column of water falls over a flat horizontal surface. Figure 3 shows a schematic view of the problem, along with the mesh proposed in this study.

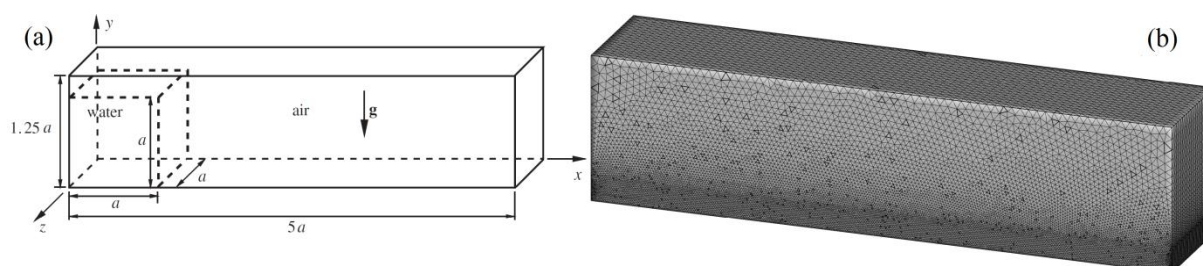


Figure 3. (a) Schematic view of the 3D broken dam problem (Lin et al. [14]) and (b) the mesh proposed by this study.

The size of the computational domain employed here is defined as $5a \times 1.25a \times a$, being $a = 0.0571504$ m, along the x , y and z directions, respectively. The mesh used consists in 1,377,120 tetrahedral elements, distributed in a non-uniform way. The boundary conditions used are a no slip wall at the bottom surface and free-slip walls at the others surfaces. The smallest element, located next to the walls, has a length of 3.94×10^{-4} m. Figure 4 shows results obtained here referring to the surge s and remaining height h , which are compared with predictions obtained experimentally by Martin and Moyce [13] and numerically by Lin et al. [14]. One can see that a good agreement is obtained with respect to the references results, especially when the water column height h is considered. Notice that a dimensionless time $t_g = (a/g)^{0.5}$ is adopted for both graphics.

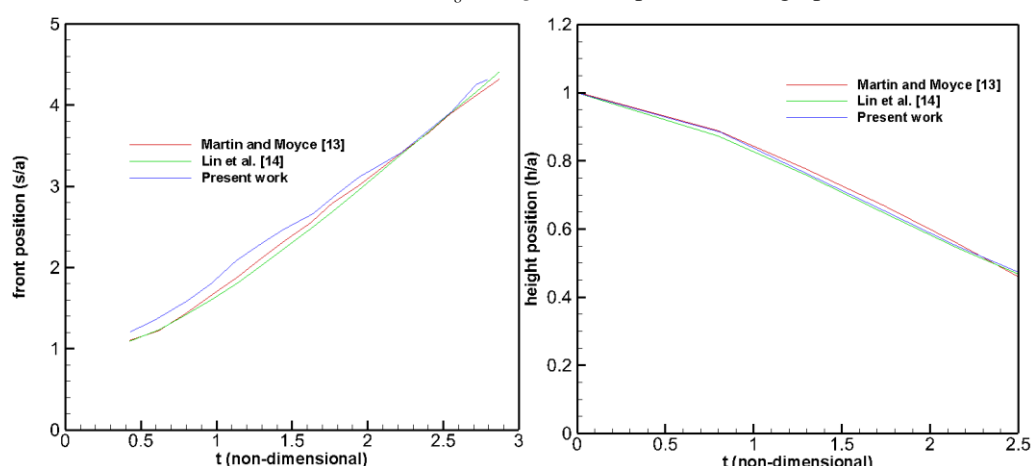


Figure 4. Surge (left) and remaining height (right) for the broken dam problem.

The evolution of the free surface over time is shown in Figure 5 for some dimensionless time instants, where it is observed that physical aspects of the flow are reproduced accurately.

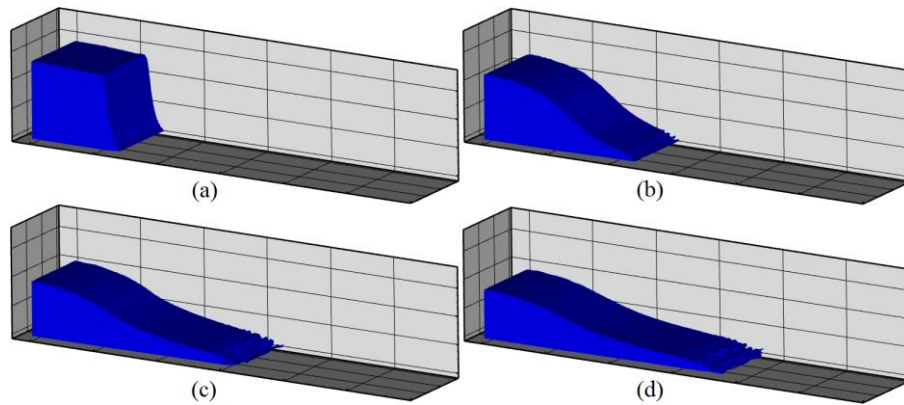


Figure 5. Free surface configurations for some dimensionless time instants: (a) $t = 0.432$; (b) $t = 1.129$; (c) $t = 1.641$; (d) $t = 1.941$.

3.2 Transient heave oscillation of a floating cylinder

The oscillation of a buoyant body on the water surface is investigated in the present application. This problem was proposed by Zandbergen et al. [15], and later studied by Donescu and Virgin [16] and Sanders et al. [5], where a circular cylinder is considered in a tank of water, with density equal to half of the water density, so that the equilibrium position corresponds to a configuration where the body is approximately half submerged. The circular cylinder presents a 2 m radius, which is released from an initial position (0.5 m above the water surface) in the middle of a tank with 100 m length and 4m depth. Free-slip conditions are imposed as boundary conditions for all the surfaces of the domain and also zero pressure for the top surface. The physical properties utilized in the present simulations are defined as follows: for the liquid phase, $\rho = 10^3$ kg/m³ is the water density and $\mu = 10^{-3}$ kg/m.s is the water viscosity; for the gaseous phase, $\rho = 1$ kg/m³ is the air density and $\mu = 2 \times 10^{-5}$ kg/m.s is the air viscosity. Information on the meshes used in this work are listed in Table 1, including the smallest element length Δx , which are localized next to the fluid-structure interface and around the free surface.

Figure 6 shows a schematic view, the details of mesh number 3 used in this study, and also the results obtained for heave (vertical displacement) decay, where one can see that predictions related to the three meshes proposed here agree very well with the numerical results presented by Donescu and Virgin [16].

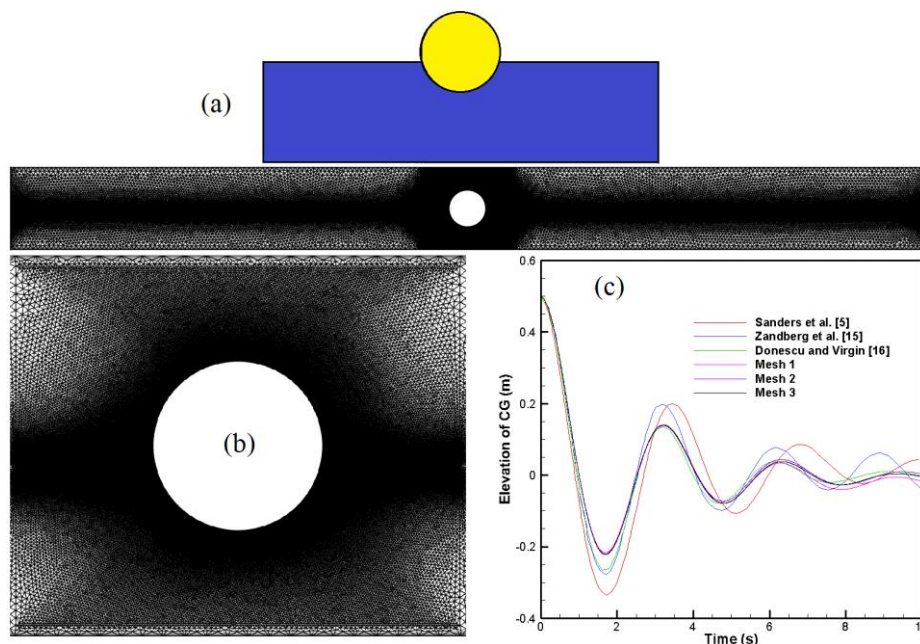


Figure 6. (a) Schematic view (based on Donescu and Virgin [16]); (b) mesh 3 details; and (c) heave decay results for the buoyant cylinder problem.

Table 1. Meshes used in the problem of floating cylinder.

Mesh	Δx (m)	Elements
1	0.0264	406,317
2	0.022	494,073
3	0.0184	602,664

3.3 Roll motion of a floating block

The present example is based on the experimental study carried out by Jung et al. [17], where a rectangular body with 0.3 m length and 0.1 m height is half submerged into a 0.9 m deep water tank and constrained to only rotate around its center of mass, as shown in Figure 7 (along with the mesh proposed by the present work). The rectangular block is released from an initial position on the water surface with a 15° angle and the tank is 10 m long. The density of the rectangular block is 1180 kg/m³. The boundary conditions used are free-slip walls at all surfaces and also zero pressure for the top surface.

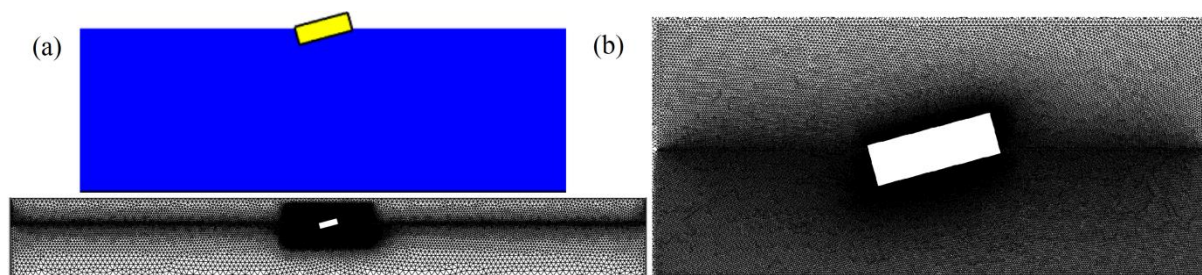


Figure 7. (a) Schematic view of the rectangular block in a water tank, initial position (Ghasemi et al. [18]) and (b) mesh proposed by the current work.

Figure 8 shows results referring to the roll angle measured over the time, where the present predictions are compared with experimental and numerical results obtained from other authors. Notice that the present simulation was carried out considering a computational mesh with 466,164 elements and smallest element length around 1.16×10^{-3} m, which are found next to the fluid-structure interface and along the free surface. One can observe that the present predictions can reproduce the period of oscillation obtained experimentally, but the amplitude of the oscillations decays faster in the experimental results. This behavior was also observed in other studies, such as Ghasemi et al. [18], Chen et al. [19], and from numerical simulations performed with the commercial software Fluent, using a mesh with 192,370 elements and smallest element length of 1.25×10^{-3} m. This smaller damping can be explained in some extent owing to the absence of extra friction damping from the physical devices used in the experiment studies (Chen et al. [19]). Other explanation may be found in the turbulent viscous dissipation, which is not fully captured in 2D simulations (Ghasemi et al. [18]).

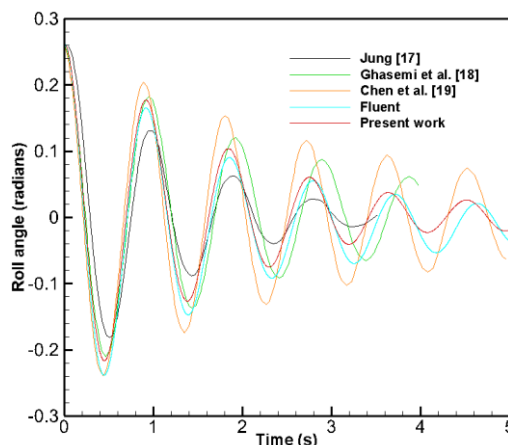


Figure 8. Rotational oscillations of a rectangular block floating in a water tank.

4 Conclusions

A finite element formulation based on the CBS Method was proposed in this work for fluid-structure applications with free-surface flows. Results obtained here demonstrate that the implemented methodology is able to reproduce complex phenomena associated with two-phase flows and their interaction with immersed structures, taking into account the good agreement observed with respect to other experimental and numerical predictions.

Acknowledgements. The authors would like to thank CNPq and CAPES for their financial support to this ongoing research. The research was developed with the support of the Núcleo Avançado de Computação de Alto Desempenho (NACAD) at COPPE, at Universidade Federal do Rio de Janeiro (UFRJ); the Centro Nacional de Processamento de Alto Desempenho em São Paulo (CENAPAD-SP); and the Laboratório Nacional de Computação Científica (LNCC).

Authorship statement. The authors hereby confirm that they are the sole liable persons responsible for the authorship of this work, and that all material that has been herein included as part of the present paper is either the property (and authorship) of the authors, or has the permission of the owners to be included here.

References

- [1] A. Biran and R. López-Pulido. *Ship Hydrostatics and Stability*. 2nd ed., Butterworth-Heinemann, 2014.
- [2] M. Karimirad, C. Michailides, A. Nematbakhsh. *Offshore mechanics: structural and fluid dynamics for recent applications*. 1st ed., John Wiley & Sons, 2018.
- [3] C. M. Wang and B. T. Wang. *Large Floating Structures: Technological Advances*. 1st ed., Springer Singapore, 2015.
- [4] R. Sharma, T. Kim, R. L. Storch, H. Hopman, S. O. Erikstad. “Challenges in computer applications for ship and floating structure design and analysis”. *Computer-Aided Design*, vol. 44, n. 3, pp. 166–185, 2012.
- [5] J. Sanders, J. E. Dolbow, P. J. Mucha and T. A. Laursen. “A new method for simulating rigid body motion in incompressible two-phase flow”. *International Journal For Numerical Methods in Fluids*, vol. 67, n. 6, pp. 713–732, 2011.
- [6] A. Calderer, S. Kang, F. Sotiropoulos. “Level set immersed boundary method for coupled simulation of air/water interaction with complex floating structures”. *Journal of Computational Physics*, vol. 277, pp. 201–227, 2014.
- [7] O. C. Zienkiewicz, R. L. Taylor, P. Nithiarasu. *The Finite Element Method for Fluid Dynamics*. 7th ed., Butterworth-Heinemann, 2014.
- [8] P. Nithiarasu, R. W. Lewis, K. N. Seetharamu. *Fundamentals of the Finite Element Method for Heat and Mass Transfer*. 2nd ed., John Wiley & Sons, 2016.
- [9] S. Osher and J. A. Sethian. “Fronts propagating with curvature-dependent speed: algorithms based on Hamilton-Jacobi formulations”. *Journal of Computational Physics*, vol. 79, pp. 12–49, 1988.
- [10] F. Pochet, K. Hillewaert, P. Geuzaine, J. Remacle, É. Marchandise. “A 3D strongly coupled implicit discontinuous Galerkin level-set based method for modeling two-phase flows”. *Computers and Fluids*, vol. 87, pp. 144–155, 2013.
- [11] M. Sussman, P. Smereka, S. Osher. “A level set approach for computing solutions to incompressible two-phase flow”. *Journal of Computational Physics*, vol. 114, pp. 146–159, 1994.
- [12] A. L. Braun. Um modelo para simulação numérica da ação do vento sobre seções de ponte. Masters dissertation, Universidade Federal do Rio Grande do Sul, 2002.
- [13] J. C. Martin and W. J. Moyce. “An experimental study of the collapse of liquid columns on a rigid horizontal plate”. *Philosophical Transactions of The Royal Society of London Series A*, vol. 244, pp. 312 – 324, 1952.
- [14] C. Lin, H. Lee, T. Lee and L. Weber. “A level set characteristic Galerkin finite element method for free surface flows”. *International Journal for Numerical Methods in Fluids*, vol. 49, pp. 521 – 547, 2005.
- [15] P. J. Zandbergen, J. Broeze, E. F. G. Van Daalen. “A panel method for the simulation of nonlinear gravity waves and ship motions”. In: J. H. Kane, G. Maier, N. Tosaka, S. N. Atluri (ed.), *Advances in Boundary Element Techniques*. Springer: Berlin, 1993, pp. 486–509.
- [16] P. Donescu and L. N. Virgin. “An implicit boundary element solution with consistent linearization for free surface flows and non-linear fluid-structure interaction of floating bodies”. *International Journal for Numerical Methods in Engineering*, vol. 51, pp. 379–412, 2001.
- [17] K. H. Jung, K. Chang and H. J. Jo. “Viscous Effect on the Roll Motion of a Rectangular Structure”. *Journal of Engineering Mechanics*, vol. 132, n. 2, pp. 190–200, 2006.
- [18] A. Ghasemi, A. Pathak and M. Raessi. “Computational simulation of the interactions between moving rigid bodies and incompressible two-fluids flows”. *Computers & Fluids*, vol. 94, pp. 1–13, 2014.
- [19] Q. Chen, J. Zang, A. S. Dimakopoulos, D. M. Kelly, C. J. K. Williams. “A Cartesian cut cell based two-way strong fluid-solid coupling algorithm for 2D floating bodies”. *Journal of Fluids and Structures*, vol. 62, pp. 252 – 271, 2016.